

Cosmol programming reproduction of explicit acceptance engine working circumstances

¹Mr. Venkateswar Rao Assistant Professor ,venkatsnmpkmm@gmail.com

²Dr. K.Suneeta Professor, kintalisuneeta@gmail.com

³Mr. V.Saidulu Assistant Professor, pecsaidulu.eee@gmail.com

Department-eee

Nagole Univeristy Engineering and Technology Hyderabad

***Abstract.** COMSOL Multiphysics software was used to simulate three-phase squirrel-cage induction motors, and some of the findings for various motor operating situations are presented in this work. For both normal operation and operation with a locked rotor, the simulation was run at the nominal rotational speed and under the nominal operating conditions described above. It is shown that the currents in the rotor bars that are closest to each other, as well as the inner torque of the motor, are all shown for each tested situation. It's possible to compare the model's simulated values of numerous motor characteristics with real-world measurements taken by the manufacturer, the manufacturer, or our lab. According to known scientific values, we may compare the simulation findings to those obtained from the actual measurements. An analogous circuit for the motor may be constructed using COMSOL and its parametric values, which can then be compared to the motor data plate and to actual testing results.*

1. Introduction

Electrical devices may be designed, studied, calculated or optimized using the Finite Element Method (FEM). Because it uses finite elements to break down a large problem into smaller pieces, the FEM is a powerful numerical approach [4]. For each element, a different set of element equations is used. Each element's single node point is where the answer may be found. COMSOL Multi Physics [5] is only one example of the several alternative FEM software options available.

For the purpose of creating a quasi-3D model, an out-of-plane thickness of the induction motor's windings was chosen in advance (opaque). Uses the AC/DC Module's Rotating

Machinery, Magnetic interface for time-domain modeling. Maxwell's equations may be efficiently solved using the magnetic vector potential and the magnetic scalar potential as dependent variables in this physical interface. Using the nodes of Ampere's Law, rotating machinery magnetic interfaces may be solved for a magnetic field in a motor (Figures 9-11).

Simulated motor parameters will be evaluated against actual data, or against theoretical hypotheses, in this study. The model will then be used to investigate the tested motor in the event of electrical or mechanical failures or abnormalities.

2. Induction Motor Design

Non-linear motor laminations have been modelled using the 800-6AM electrical steel. The With this material, you may simulate stator and rotor lamination in COMSOL using the B-H curve. Anisotropic equivalent conductivity may be calculated using homogenization methods because of the laminations [12],[3] and [4].

The following are the homogenization formulae used in this study:

$$\sigma_x = \sigma_y = \sigma, \tag{1}$$

$$\sigma = \frac{1}{n^2} \sigma, \tag{2}$$

Note that the values of the simulated parameters depend on the accuracy of the identification and computation of the model's parameters, the machine's shape and material properties, precise meshing, especially of the motor air gap, and the simulation's time step.

End winding impedance components for feeding an induction motor from a sinusoidal three-phase sinusoidal voltage source were coupled to Comsol's Electrical Circuit interface. In addition to the external rotor circuits [8, 5], and 6 that are developed, this interface is employed. This equation calculates stator resistance for overhang, R_{Send} , and an iron rotor bar. The following are the equations:

$$R_{Send} = \rho \frac{2l_0 N_s}{}, \tag{3}$$

A

Area of the stator winding (m²), cage end-ring diameter (m), stator phase number (NS), and the cage end-ring area (AR) (m²), where l_0 is the average stator winding overhang (m) (m²).

3. Nominal Operating Condition Modeling and Analysis

As shown in Tab 1, the catalog parameters have been used to model the induction motor's performance. Changes were made to COM-Rotating SOL's Machinery, Magnetic physics section to alter the motor speed. The induction motor's geometry may be seen in the figure above (Figure 1).

Tab. 1: The motor's chosen settings.

Parameter	Value	Parameter	Value
The wattage	4 kW	Theoretical power ratio	0.83
Value of voltage at the unitary value	400 V	Nominal velocity	1440 rpm
Symbolic current	8.4 A	Torque at a given speed	27 N·m
Initiating current to voltage	6	The ratio of starting torque to total torque	2.7
The average number of occurrences	50 Hz	Efficiency at a minimum level.	83.1

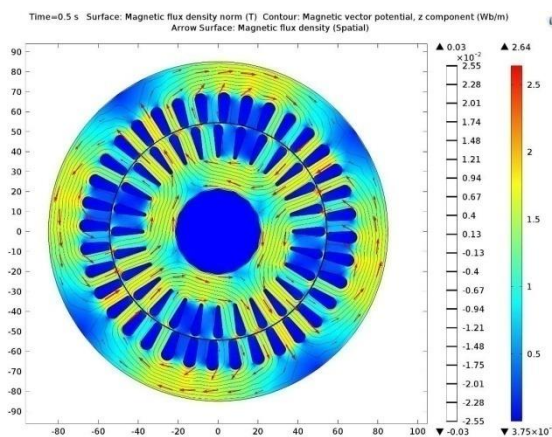
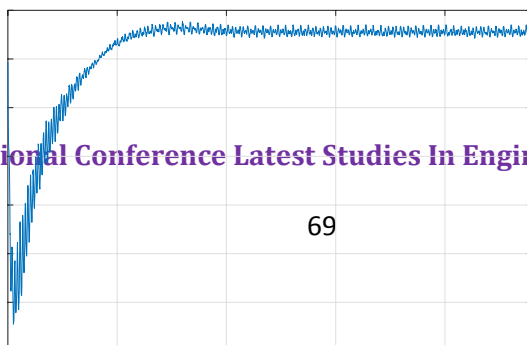


Fig. 1: Vector potential lines of magnetic flux density and equi-potentials



Locked Rotor Condition Motor Simulation

At zero revolutions per minute, the simulation was run in Rotating Machinery, Magnetic Physics, with a locked rotor state. Magnetic flux density and vector potential lines at nominal supply voltage are shown in Figure 11. High currents in the rotor cage drive the rotor flux toward the air gap. As a result, the flux tends to accumulate around the rotor's surface and between its slots, where it gets saturated. Under normal operating circumstances, as seen in Figure 2, the motor's rotor iron has a low magnetic flux density.

During the simulation, the temperature of the laboratory was taken into consideration. Assuming that the motor temperature is equal to ambient, the stator current and catalog starting current are compared.

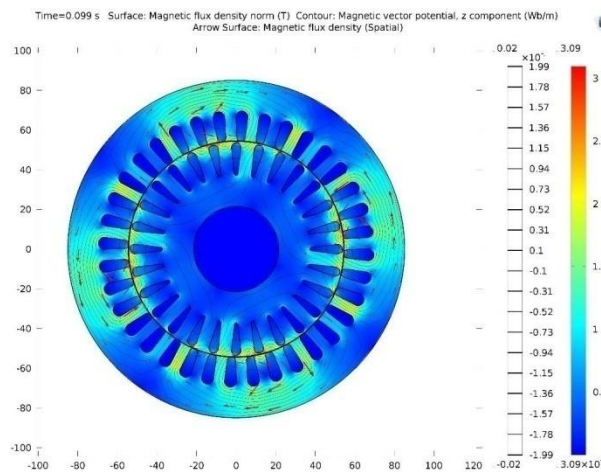


Fig. 11: Under a locked rotor at the nominal supply voltage and magnetic flux density, equipotential lines of magnetic vector potential may be generated

An electric motor's inner torque and other information, as shown in the figures in Figures 12,

13, 14, and 15, were derived from the simulation results (Fig. 12). Harmonic analysis results are compared to the short-circuit characteristic and the initial current in Table 4 of the motor catalog.

Tab. 4: A comparison of the current flowing through the stator while the rotor is locked.

Source	Stator current
A list of motors	50.4 A
The manufacturer's price	54.83 A
Simulation	55.5 A

Based on the results of COMSOL Analysis

Without accounting for iron loss, this is an induction motor steady state harmonic equivalent circuit. Besides R1 and L1, there are two further components to the stator phase resistance: R1 and L1.

$$R_1 = R_{Send} + R_{sfem} \tag{15}$$

$$L_{1\sigma} = L_{Send} + L_{\sigma sfem} \tag{16}$$

The first section of Eq. (15) and Eq. (16) combines Eq. (3) and Eq. (9). 2D field model in second portion. When COM-SOL is asked to compute RSfem, the slots are provided as multi-turn coil domains. Emotional Intelligence (16).

Tab 5 compares predicted motor parameters to those obtained from the motor data plate and observed values.

Tab. 5: A comparison of the induction motor's operating parameters.

	From the information on the data plate.	As a result of the data collected	From COMSOL
R_1 (Ω)	3.08	3.02	2.96
$L_{1\sigma}$ (mH)	2.8	3.1	3.08
L_m (mH)	138	140	125
R_2 (Ω)	1.22	1.22	1.38
$L_{2\sigma}$ (mH)	2.8	3.1	3.08

6. Conclusion

Simulated results for induction motor model's nominal operating state are quite comparable

to catalog values and observed values of actual motor operation, to be more precise. Table 2 shows very slight differences between the simulated and actual stator current and torque values for the nominal operating state.

If the parameters utilized in the model have been correctly identified and calculated, the geometry and material properties of the machine, the precise meshing, particularly of the motor air gap, and an appropriate time step are all factors that influence the simulated parameters.

References

1. DE GERSEM, H., K. HAMEYER and T. WEI- LAND. Field-circuit coupled models in elec- tromagnetic simulation. *Journal of Com- putational and Applied Mathematics*. 2004, vol. 168, iss. 1–2, pp. 125–133. ISSN 0377-0427. DOI: 10.1016/j.cam.2003.05.008.
2. ZHOU, P., D. LIN, W. N. FU, B. IONESCU and Z. J. CENDES. A general cosimula- tion approach for coupled field-circuit prob- lems. *IEEE Transactions on Magnetics*. 2006, vol. 42, iss. 4, pp. 1051–1054. ISSN 0018-9464. DOI: 10.1109/TMAG.2006.871374.
3. GRECONICI, M., C. KOCHR and G. MADE- SCU. Advantages of FEM analysis in electri- cal machines optimization used in wind en- ergy conversion systems.
4. NIKISHKOV, G. P. *An Introduction to the Finite Element Method*. 3rd ed. New York: McGraw-Hill, 2006. ISBN 978-0-0724-6685-0.
5. COMSOL Multiphysics. *Reference manual*. New York: COMSOL Multiphysics, 2013.
6. COMSOL Multiphysics. *AC/DC Module User's Guide*. New York: COMSOL Multiphysics, 2013.
7. ESCARELA-PEREZ, R., E. MELGOZA and
8. J. ALVAREZ-RAMIREZ. Systematic Coupling of Multiple Magnetic Field Systems and Circuits Us- ing Finite Element and Modified Nodal Anal- yses. *IEEE*

- Transactions on Magnetics. 2011, vol. 47, iss. 1, pp. 207–213. ISSN 1941-0069. DOI: 10.1109/TMAG.2010.2087387.
9. KOCMAN, S., P. ORSAG and P. PECINKA. Multiphase electric machines for variable-speed applications. Simulation of Start-Up Behaviour of Induction Motor with Direct Online Connection. 2017, vol. 15, iss. 5, pp. 754–762. ISSN 1336-1376. DOI: 10.15598/aece.v15i5.2342.
10. MARTINEZ, J., A. BELAHCEN and
11. ARKKIO. A 2D FEM model for transient and fault analysis of induction machines. Przegląd Elektrotechniczny. 2012, vol. 2012, no. 7b, pp. 157–160. ISSN 2449-9544. DOI: 10.1109/TIE.2008.918488.
12. SAVOV, V. N., Z. D. GEORGIEV and E. S. BOGDANOV. Analysis of cage induction motor by means of the finite element method and coupled system of field, circuit and motion equations. Electrical Engineering. 1997, vol. 80, iss. 1, pp. 21–28. ISSN 1432-0487. DOI: 10.1007/BF01235666.